Heliyon 8 (2022) e09620

Contents lists available at ScienceDirect

Heliyon

journal homepage: www.cell.com/heliyon

Research article

Effect of maximum density and internal heating on the stability of rotating fluid saturated porous layer using LTNE model

N.K. Enagi [a,b], Krishna B. Chavaraddi [c,*], Sridhar Kulkarni [d], G.K. Ramesh [e]

[a] University: Research and Development Centre, Bharathiar University, Coimbatore-641046, India
[b] Department of Mathematics, KRCE Society's GGD Arts, BMP Commerce and SVS Science College, Bailhongal-591102, India
[c] Department of Mathematics, S.S. Government First Grade College & P.G. Studies Center, Nargund-582207, India
[d] Department of Mathematics, Government First Grade College, Gokak-591307, India
[e] Department of Mathematics, K.L.E. Society's J.T. College, Gadag-582101, India

ARTICLE INFO

Keywords:
Convection
Density maximum
Internal heat generation
Thermal non-equilibrium

ABSTRACT

The impact of heat generated inside the porous layer containing a fluid and density maximum when the porous structure is studied analytically subjected to rotation for the case of unlike temperatures of both solid and fluid phases. Two equations each representing solid and fluid phases are used as energy equations. The linear stability theory is used and is based on normal mode technique. Galerkin method is used to find the Eigen values of the problem. The rotation of the porous layer provides extra strength to the system, protecting the structure from instability, however internal heat generation does not support the system in retaining its strength, causing the system to destabilize. Both the conductivity ratio and the density function have a negative impact on system stability. Consequently, the rotation parameter *Ta* stabilizes the system, whereas internal heat generation, conductivity ratio, and density function destabilizes the onset of convection.

1. Introduction

Convective heat transfer is one of the most influenced and powerful mechanism. The study of convective heat transfer in a porous medium containing fluid has gained much attention in these days, because of its vital importance in extraction of energy from the surface of the earth. It is found that in most of the cases the source of heat is generated by taking itself which leads to setting up of convection by the generation of heat inside the layer. In most of natural and practical context in which convection is managed by internal heat sources. Hence the study of internal heat generation acquired much significance, because its applications include the storage of radioactive materials, geophysics and combustion.

Nield and Bejan [1] have introduced a model of energy which has two equations is called a two-fluid model. Rees [2, 3] in his paper studied through a porous medium when the solid and fluid phases have different temperatures. Govender and Vadasz [4] examined stability of anisotropic rotating, driven convection in the layer. The most important investigation on thermal stability in porous media is well documented by Banu and Rees [5] and Malashetty et al. [6, 7, 8, 9, 10]. Postelnicu [11] has been investigated the stability of convection by using Darcy-Brinkman model. Kuznetsov et al. [12] all have analyzed how the convection in nanofluid saturated in the permeable medium is affected when both fluid and solid phases have different temperature.

Yekasi et al. [13] has explored the characterization of heating inside on Rayleigh-Benard convection driven by suction-injection combination by considering free rigid boundary. Bhaduria et, al [14] investigated how the time periodic gravity modulation with inside heating on Rayleigh-Benard convection in vertically oscillating micro polar fluid. A detailed study on thermal non-equilibrium model has been carried out by Shivakumara et al. [15, 16, 17, 18, 19, 20, 21, 22]. Dhananjay Yadav et al. [23] examined the effect of inner heating and rotating layer using Darcy–Brinkman model and conclude that rotation inhibits the system. Sarvanan [24] has studied the nature of internal heat generation and maximum density function and

* Corresponding author.
E-mail address: ckrishna2002@yahoo.com (K.B. Chavaraddi).

https://doi.org/10.1016/j.heliyon.2022.e09620
Received 20 November 2021; Received in revised form 2 January 2022; Accepted 27 May 2022

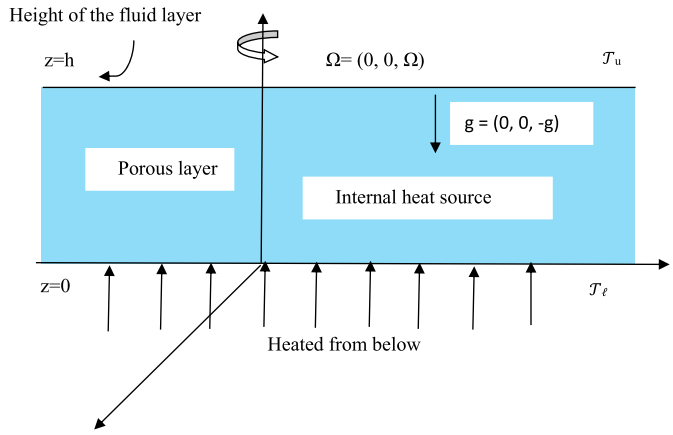

Fig. 1. Physical configuration.

shows that both the parameters enhance the stability of the system. Gaseer et al. [25] studied the effect interior heating for the onset of convection. Chavaraddi et al. [26] gave a conclusion that the couple stress, rotation and thermal anisotropy parameters are stabilizing the onset of convection in a saturated medium. Lotten and Rees [27] studied the anisotropy and heat generated inside in an inclined layer. Israel-Cookey and Omubo-Peppl [28] studied the stability in a low Prandtl number fluid with heating process inside the structure. Srivastava et al. [29] examined the onset of thermal magneto convection in an anisotropic loosely pack medium. Postelnicu [30] studied the effect of inertia on the onset of mixed convection in LTNE medium. Xu et al. [31] focuses on various flow and heat transfer modes of nanofluid, metal foam and the combination of the two, with the physical properties of nanofluid and metal foam summarized. Oumar et al. [32] have been studied the onset of Rayleigh-Benard electro-convection in a micro polar fluid with internally heating particles. A new fractal theoretical model with periodic pore morphology, which idealizes the pore channels of the porous media as gourd-shaped structure, is established to model the transport in complex porous media by Wu et al. [33]. Xu [34] investigated the theoretical study of the fully-developed forced convection heat transfer in a microchannel partially filled with a porous medium core is performed by considering the local thermal non-equilibrium (LTNE) effect between the solid and fluid phases. Anwar Ahmed Yousif et al. [35] investigated the impact of using triple adiabatic obstacles on natural convection inside porous cavity under non-Darcy flow and local thermal non-equilibrium model. Omar Rafae et al. [36, 37, 38] examined the simulation of complete liquid–vapor phase change process inside porous evaporator using local thermal non-equilibrium model.

In most of the situations it is observed that temperature fields of solid and fluid phase of the porous medium are assumed to be identical such a situation is generally known as local thermal equilibrium (LTE). However, in many practical situations involving porous material and also media in which there is a large temperature difference between the fluid and the solid phases, it has been realized that the assumption of LTE model is inadequate for proper understanding of the heat transfer problems. In such circumstances the local thermal non-equilibrium (LTNE) effects are to be taken into consideration in which case the single energy equation has to be replaced by two, one for each phase. The main objective of present paper is to study the effect of maximum density and internal heating on the stability of rotating fluid using LTNE model.

2. Mathematical model

In this paper, we consider a porous media of height 'h' which is extended horizontally between two free surfaces and the fluid is subjected to rotation. Let T_ℓ and $\mathcal{T}_u$ be the temperatures at the lower and upper surfaces. The temperature gradient $\nabla\mathcal{T} = \mathcal{T}_\ell - \mathcal{T}_u$ is uniform and $\mathcal{T}_\ell > \mathcal{T}_u$ maintained between the two surfaces. A momentum expression contains the time derivative term and two separate equations are used for temperature. This physical model is shown in Fig. 1.

$$\nabla \cdot \mathrm{q} = 0 \tag{1}$$

$$\frac{1}{\varepsilon}\frac{\partial q}{\partial t} + \frac{2}{\varepsilon}\Omega \times q = -\frac{1}{\rho_o}\nabla p + \frac{\rho}{\rho_o}g - \frac{v}{k}q \tag{2}$$

$$\varepsilon\left(\rho_c\right)_f \frac{\partial T_f}{\partial t} + \left(\rho_c\right)_f (q\cdot\nabla)\mathcal{T}_f = \varepsilon k_f \nabla^2 \mathcal{T}_f + h\left(\mathcal{T}_s - \mathcal{T}_f\right) + \varepsilon q_f \tag{3}$$

$$(1-\varepsilon)\left(\rho_c\right)_s \frac{\partial T_s}{\partial t} = (1-\varepsilon)k_s\nabla^2\mathcal{T}_s - h\left(\mathcal{T}_s - \mathcal{T}_f\right) + (1-\varepsilon)q_s \tag{4}$$

$$\rho = \rho_0[1 - \beta_1\left(\mathcal{T}_f - \mathcal{T}_u\right) - \beta_2\left(\mathcal{T}_f - \mathcal{T}_u\right)^2 \tag{5}$$

To remove the pressure term from the momentum equation (2) and making equations (3) and (4) dimensionless by using eq. (5) and following transformations (6):

$$\left.\begin{aligned} &(x,y,z) = d\left(x^*,y^*,z^*\right) \qquad (u,v,w) = \frac{\varepsilon k_f}{(\rho_c)_f d}\left(u^*,v^*,w^*\right) p = \frac{k_f\mu}{(\rho_c)_f K}p^*, \\ &\mathcal{T}_f = \left(\mathcal{T}_l - \mathcal{T}_u\right)\mathcal{T}_f^* + \mathcal{T}_u, \quad \mathcal{T}_s = \left(\mathcal{T}_l - \mathcal{T}_u\right)\mathcal{T}_s^* + \mathcal{T}_u, \quad t = \frac{(\rho_c)_f d^2}{k_f}t^* \end{aligned}\right\} \tag{6}$$

$$\frac{1}{P_{rD}}\frac{\partial}{\partial t}(\nabla^2 w) + (T_a)^{1/2}\frac{\partial^2 w}{\partial z^2} = R_1\nabla_1^2\mathcal{T}_f + R_2\nabla_1^2\mathcal{T}_f^2 - \nabla_1^2 w - \frac{\partial^2 w}{\partial z^2} \tag{7}$$

$$\frac{\partial T_f}{\partial t} + w\frac{\partial^2 T_f}{\partial z^2} = \nabla_1^2 \mathcal{T}_f + \frac{\partial^2 T_f}{\partial z^2} + H\left(\mathcal{T}_s - \mathcal{T}_f\right) + Q_f \tag{8}$$

$$\alpha\frac{\partial T_s}{\partial t} = \nabla_1^2 \mathcal{T}_s + \frac{\partial^2 T_s}{\partial z^2} - \gamma H\left(\mathcal{T}_s - \mathcal{T}_f\right) + Q_s \tag{9}$$

$$R_A = \beta_1 \rho_0 g h (\rho_c)_f \left(\mathcal{T}_l - \mathcal{T}_u\right) K/\varepsilon\mu k_f, \qquad R_M = \beta_2 \rho_0 g h (\rho_c)_f \left(\mathcal{T}_l - \mathcal{T}_u\right)^2 K/\varepsilon\mu k_f \tag{10}$$

Here Eq. (10) is the Rayleigh number corresponding to the properties of fluid phase.
Here R_M serves as a measure of the density maximum and when to begin property.

$$H = hd^2/(1-\varepsilon)k_s, \text{ the non-dimensional interphase heat transfer coefficient} \tag{11}$$

$$Ta = 2\Omega\rho_o K/\varepsilon\mu, \text{ the Taylor number} \tag{12}$$

$$\gamma = \varepsilon k_f/(1-\varepsilon)k_s, \text{ the conductivity ratio} \tag{13}$$

$$\alpha = (\rho_c)_s k_f/(\rho_c)_f k_s, \text{ the diffusivity ratio} \tag{14}$$

$$Q_f = q_f/\left(\mathcal{T}_l - \mathcal{T}_u\right)k_f, \text{ the fluid phase internal heat generator parameter} \tag{15}$$

$$Q_s = d^2 q_s/\left(\mathcal{T}_l - \mathcal{T}_u\right)k_s \text{ solid phase internal heat generator parameters} \tag{16}$$

where Eqs. (11)-(13) are Taylor number, conductivity ratio and diffusivity ratio respectively.

2.1. Quiescent state

The basic state is assumed to be quiescent and is given by

$$u = v = w = 0 \qquad \mathcal{T}_f = \mathcal{T}_{fb}(z) \qquad \mathcal{T}_s = \mathcal{T}_{sb}(z) \tag{17}$$

The temperature of fluid phase and solid phase satisfies the equations

$$\frac{d^2 T_{fb}}{dz^2} = -Q_f, \qquad \frac{d^2 \mathcal{T}_{sb}}{dz^2} = -Q_s \tag{18}$$

$$\text{with the boundary conditions } \mathcal{T}_{fb} = \mathcal{T}_{sb} = 1 \text{ at } z = 0 \; \mathcal{T}_{fb} = \mathcal{T}_{sb} = 0 \text{ at } z = 1 \tag{19}$$

So that the steady state solutions are given by

$$T_{fb} = -\frac{Q_f}{2}z^2 + \left(\frac{Q_f}{2} - 1\right)z + 1, T_{sb} = -\frac{Q_s}{2}z^2 + \left(\frac{Q_s}{2} - 1\right)z + 1 \tag{20}$$

2.2. Perturbed state

The basic state is perturbed and quantities in the perturbed state are given by

$$(u, v, w) = \left(u^1, v^1, w^1\right), \quad q = q^1, \quad \mathcal{T}_f = \mathcal{T}_{fb} + \theta, \quad \mathcal{T}_s = \mathcal{T}_{sb} + \varphi \tag{21}$$

Substituting equation (21) into (7) to (9) and using equation (20) we obtained following linearized equations for perturbed quantities (after neglecting the primes)

$$\frac{1}{P_{rD}}\frac{\partial}{\partial t}(\nabla^2 w) + (T_a)^{1/2}\frac{\partial^2 w}{\partial z^2} = R_A\nabla_1^2\theta + 2R_M\left\{-Q_f\frac{z^2}{2} + \left(\frac{Q_f}{2} - 1\right)z + 1\right\}\nabla_1^2\theta - \nabla_1^2 w - \frac{\partial^2 w}{\partial z^2} \tag{22}$$

$$\frac{\partial\theta}{\partial t} + w\left(-Q_f z + \frac{Q_f}{2} - 1\right) = \nabla_1^2\theta + \frac{\partial^2\theta}{\partial z^2} + H(\varphi - \theta) \tag{23}$$

$$\alpha\frac{\partial\varphi}{\partial t} = \nabla_1^2\varphi + \frac{\partial^2\varphi}{\partial z^2} - \gamma H(\varphi - \theta) \tag{24}$$

Since the fluid and solid phases are not in thermal equilibrium, the use of appropriate thermal boundary condition may pose a difficulty. However, the assumption that the solid and fluid phases have equal temperatures at the boundary surfaces made at the beginning of this section helps in overcoming this difficulty. Accordingly, equations (22) to (24) are solved impermeable isothermal boundaries. Hence the boundary conditions are

$$\omega = \frac{\partial\omega}{\partial z} = \theta = \varphi = 0 \text{ at } z = 0, 1 \tag{25}$$

2.3. Linear stability analysis

To study the linear stability theory, we use the linearized version of equations (22) to (24). The principle of exchange of stabilities holds in the presence of isotropy and non-LTE effects (there is only one destabilizing agency) so that the onset of convection is stationary (i.e. $\omega = 0$). We seek the solutions to the linearized equations in the form

$$[w, \theta, \varphi] = [W(z), \Theta(z), \Phi(z)]\, e^{i(lx+my)\sin\pi z+\omega t} \tag{26}$$

Here l, m is the wave numbers in horizontal plane and ω is growth rate. Infinitesimal perturbation of the rest state may be either damp or grow depending on the values of the parameter ω. Substituting the equations (25) in the equations (22) to (24) we get the following equations

$$\left[\frac{\omega}{Pr_D}(a^2 - D^2) - (Ta)^{1/2} D^2 + (a^2 - D^2)\right] W - \left[R_A + 2R_M\left\{-\frac{Q_f}{2}z^2 + \left(\frac{Q_f}{2} - 1\right)z + 1\right\}\right] a^2\Theta = 0 \tag{27}$$

$$\left(-Q_f z + \frac{Q_f}{2} + 1\right) W + \left(\omega + a^2 + H - D^2\right)\Theta - H\Phi = 0 \tag{28}$$

$$\gamma H\Theta + \left(\alpha\omega + a^2 + \gamma H - D^2\right)\Phi = 0 \tag{29}$$

The eigenvalue problem associated with the equations (27)–(29) in a horizontal fluid layer bounded by two rigid walls, governing the stability of the basic motion against normal mode perturbations, deduced has the form. We use Galerkin's technique to solve the Eigen value problem. In the Galerkin approach used here the basis (trial) functions satisfy the boundary conditions. In this case, the simplest choice seems to be to write W, Φ and Θ as

$$W_1 = z^3(1-z)^2, \quad \Theta = \Phi = z(1-z) \tag{30}$$

With this choice (30), the unknown functions W, ϕ and Θ satisfy the boundary conditions (25) and integrating the equations, so obtained over the layer from 0 to 1, we get

$$\left[\frac{a^2}{66} + \left\{(Ta)^{\frac{1}{2}} + 1\right\}\frac{2}{9}\right] A_1 - \left[\frac{R_A}{2} + R_M\left\{\frac{Q_f + 14}{36}\right\}\right] a^2 B_1 = 0 \tag{31}$$

$$\left(18 - Q_f\right) A_1 - 168(a^2 + H + 10)B_1 + 168HC_1 = 0 \tag{32}$$

$$-\gamma H B_1 + (a^2 + \gamma H + 10)C_1 = 0 \tag{33}$$

Now to solve R_A the above equations (31)-(33) can be put in the form of the following matrix, we get

$$\begin{bmatrix} \frac{a^2}{66} + \{(Ta)^{1/2} + 1\}\frac{2}{9} & -\left[R_A + R_M\left\{-\frac{Q_f}{2}z^2 + \left(\frac{Q_f}{2} + 1\right)z + 1\right\}\right] a^2 & 0 \\ 18 + Q_f & -168\left(a^2 + H + 10\right) & 168H \\ 0 & -\gamma H & a^2 + \gamma H + 10 \end{bmatrix} \begin{bmatrix} A_1 \\ B_1 \\ C_1 \end{bmatrix} = \begin{bmatrix} 0 \\ 0 \\ 0 \end{bmatrix} \tag{34}$$

By setting the determinant of the coefficient matrix (34) to zero, we get

$$R_A = \frac{448(a^2 + 10)}{a^2(18 + Q_f)}\left[\frac{a^2}{22} + \{(Ta)^{1/2} + 1\}\frac{2}{3}\right]\left[1 + \frac{H}{a^2 + \gamma H + 10}\right] - \frac{2}{9}R_M(Q_f + 14) \tag{35}$$

3. Result analysis

The impact of internal heating and density maximum in a rotating Darcy-Brinkman porous medium of convection has been investigated using Galerkin method. This study is concentrated to steady state of convection because oscillatory mode seems to be highly implausible. Rayleigh number Eq. (35) is used to determine the stability of the system. If the Rayleigh number is below or above the critical value then the flow is laminar or turbulent. Figs. 2(a) to 2(e) shows that the marginal curves are connected in topological sense and thus the linear stability is calculated in terms of critical Rayleigh number. The system is stable below this critical Rayleigh number and unstable above this number. Figs. 2(a) and 2(e) show the graph of neutral curves for different values of Ta, N, Q_f, R_M, and γ. We observe that there is no change in the topological connectedness of the curves which shows the neutral nature of these curves. Figs. 3(a) to 3(c) exhibit the effect of N against critical Rayleigh number R_A for distinct values of γ, Ta and Q_f. Figs. 3(a) and 3(c) discloses that R_A is decreasing with increase in γ, and Q_f, as N represents the transfer of heat between the fluid and solid phases. If N is very small indicates that there is almost zero transfer of heat between the two phases on the other hand if N is very large indicates there is a rigorous transfer of heat between the two phases. The behavior of the critical Raleigh number points out that the effect of conductivity ratio and internal heat generator of fluid phase is to destabilize the onset of convection. This is because when the conductivity ratio increases the fluid part of the medium gains more heat from the solid phase which leads to begin the convection sooner and thereby, the critical Rayleigh number decreases. When the critical Rayleigh number decreases it implies that the system is coming closer to destabilized mode. The same effect is observed for the case of internal heat generation which is shown in Fig. 3(b). The increase in the internal heat generation causes the fluid phase to acquire more heat and thus convection starts early. It is also noted that R_A is independent of γ when heat transfer is very less and independent of N when γ is very large (≥10). Fig. 3(b) shows the effect of Ta versus N on Critical Rayleigh number. It is found that when rotation increases, the values of R_A rise, demonstrating that rotation of fluid has the impact of improving the system's stability. The reason is as the rotation of the porous layer increases there is a slow distribution of heat in the porous layer and fluid particles get heated slowly thus there is a delay in onset of convection which shows that the system is in stable condition.

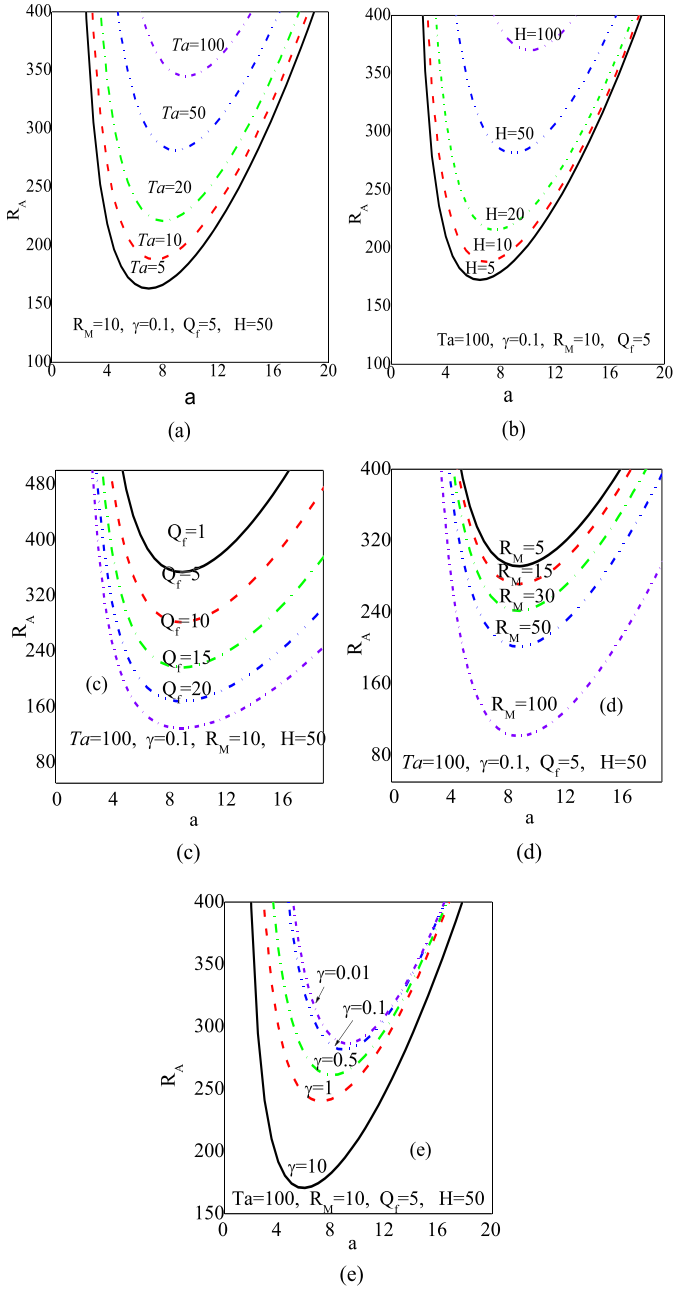

Fig. 2. (a): Neutral stability curves Vs 'a' for different values of *Ta*. (b): Neutral stability curves Vs 'a' for different values of H. (c): Neutral stability curves Vs 'a' for different values of Q_f. (d): Neutral stability curves Vs 'a' for different values of R_M. (e): Neutral stability curves Vs 'a' for different values of γ.

Figs. 4(a) and 4(b) display the variation of 'a' against N for distinct values of γ and Ta. In Fig. 4(a) it is detected that, for small and large value of N, the critical wave number is not depending on the values of γ. But for intermediate values the critical wave number increase with decrease in γ and attains a maximum. Fig. 4(b) the critical wave number curves increase with increase in Ta, signifying that the impact of Ta is to improve the system stability.

Figs. 5(a) to 5(d) demonstrate the variation of R_A against Q_f for various values of γ, Ta, N and R_M. In Fig. 5(a) the effect of γ on R_A is displayed. It is found that R_A decreases with increase in γ, which shows that the conductivity ratio γ destabilizes the system. In Fig. 5(b) the effect of Ta on the R_A is revealed. It is detected that the R_A increases with increase in Ta, representing that the Taylor number has stabilizing effect. In Fig. 5(c) appear that the effect of Q_f on R_A is presented for various values of N. It is noted that the growing values in Q_f, the values of R_A decline and become zero at some finite value of Q_f. This shows that the Q_f quickens the onset of convection and thus the effect of Q_f causes the instability of the system. In Fig. 5(d) depicted that the R_A decreases as the R_M increases, which indicating that the system turns into unstable mode due to effect of density function.

The comparison presented in Figs. 6(a) and 6(b) is the critical Rayleigh number graphs of present study with the case of Darcy–Benard convection (see Banu and Rees [5]).

Figs. 6(a) and 6(b) are very good comparison of critical Rayleigh numbers with the case Darcy-Benard convection studied by Banu and Rees [5].

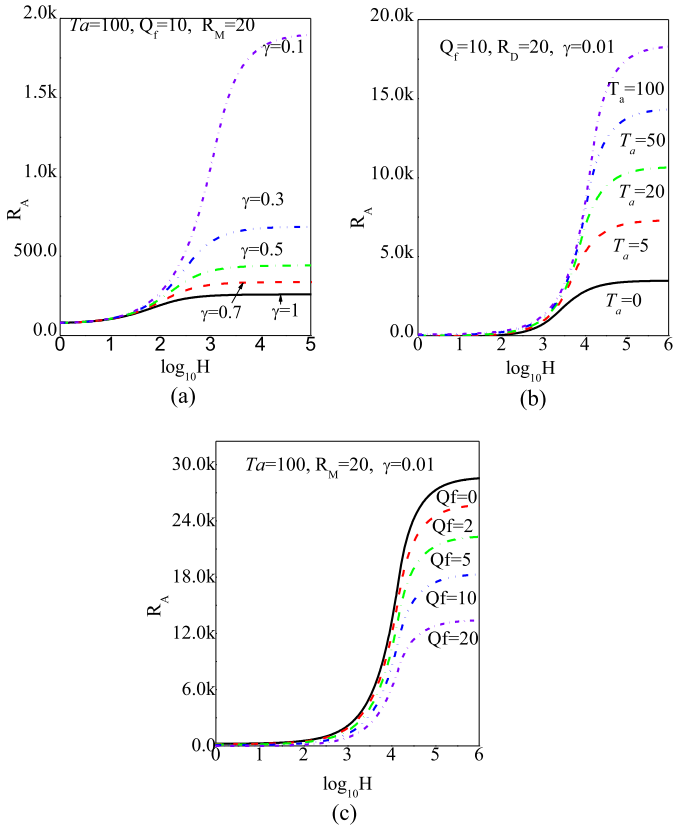

Fig. 3. Variation of R_A against H for different values of γ. (b): Variation of R_A against H for different values of *Ta*. (c): Variation of R_A against H for different values of Q_f.

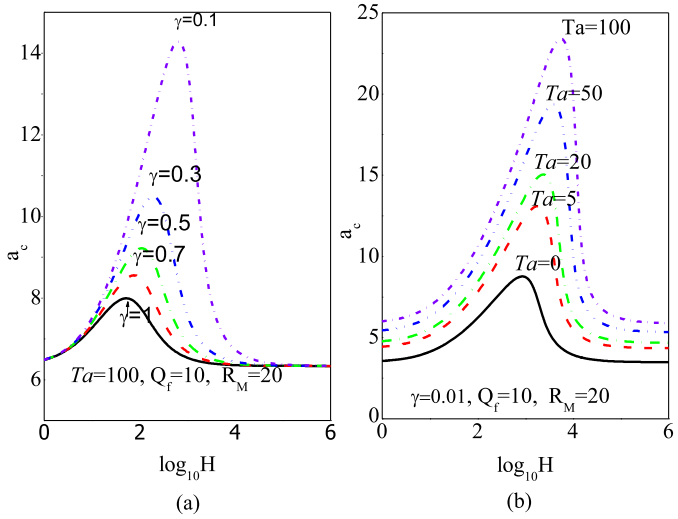

Fig. 4. (a): Variation of 'a' against 'H' for different values of γ. (b): Variation of 'a' against 'H' for different values of *Ta*.

The comparison of critical wavenumber graphs of present study with Darcy–Benard convection done by Banu and Rees [5] is given in Figs. 6(c) and 6(d).

The critical wavenumbers in Figs. 6(c) and 6(d) show the good comparison with the work done by Banu and Rees [5]. Also, the results obtained are presented in Tables 1 and 2, shows a favorable agreement of present work with the results of Banu and Rees [5] in the absence of rotation, internal heat generation and maximum density function thus give confidence that the numerical results obtained are accurate.

4. Conclusion

The stability of a fluid saturated rotating porous layer with internal heat generation and density maximum is studied when both fluid and solid phases have different temperatures. Galerkin method is used to find the Eigen values of the problem. The effect of internal heat generation, rotation and conductivity ratio is determined and demonstrated graphically. The following conclusions have been drawn point by point:

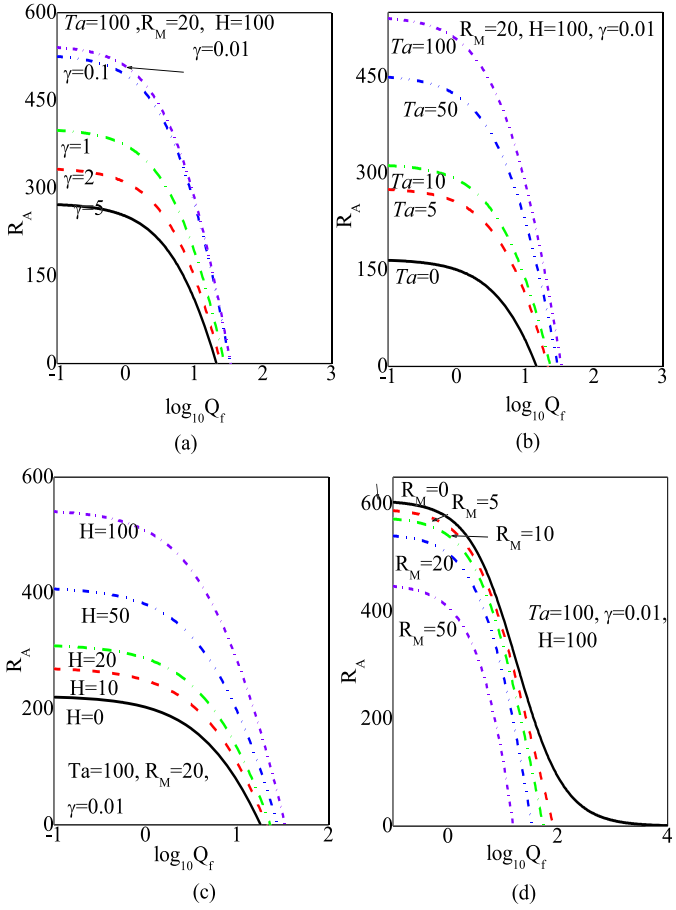

Fig. 5. (a): Plots of R_A versus Q_f for different values of γ. (b): Plots of R_A versus Q_f for different values of Ta. (c): Plots of R_A versus Q_f for different values of H. (d): Plots of R_A versus Q_f for different values of R_M.

Table 1. Comparison of the critical Rayleigh number of present study with the case of Darcy–Benard convection done by Banu and Rees [5] in the absence of rotation, internal heat generation and maximum density function.

Variation of critical Rayleigh number versus logH for specific values of γ								
H	Critical Rayleigh number obtained for the case of present study				Critical Rayleigh number obtained by Banu and Rees [5]			
	$\gamma = 0.1$	$\gamma = 0.3$	$\gamma = 0.5$	$\gamma = 1$	$\gamma = 0.1$	$\gamma = 0.3$	$\gamma = 0.5$	$\gamma = 1$
-2	39.50864	39.50863	39.50863	39.50863	39.50871	39.50870	39.50870	39.50870
-1	39.69856	39.69833	39.69811	39.69755	39.68835	39.68815	39.68795	39.68745
0	41.56690	41.54569	41.52491	41.47464	41.45493	41.43599	41.41741	41.37239
1	58.14440	56.70393	55.43970	52.90179	57.06386	55.79444	54.66823	52.37010
2	163.2115	118.4482	96.35335	72.67197	156.4227	116.2631	95.33384	72.35688
3	370.3745	163.3230	115.6035	78.24936	366.9394	162.8960	115.4474	78.21098
4	427.0948	170.2972	118.1683	78.90134	426.6959	170.2506	118.1551	78.89954
5	433.6257	171.0306	118.4330	78.96766	433.5968	171.0312	118.4350	78.96963
6	434.2889	171.1044	118.4596	78.97430	434.2979	171.1091	118.4630	78.97663
7	434.3553	171.1118	118.4623	78.97497	434.3680	171.1169	118.4658	78.97733
8	434.3620	171.1125	118.4625	78.97503	434.3750	171.1176	118.4661	78.97740
9	434.3627	171.1126	118.4626	78.97504	434.3757	171.1177	118.4661	78.97741
10	434.3627	171.1126	118.4626	78.97504	434.3758	171.1177	118.4661	78.97741

- The rotation of the porous layer if offering extra strength to the system thereby protecting the structure from instability, whereas the internal heat generation does not support the system in maintaining its strength and thus takes the system from a safe zone to a dangerous zone of destabilization.
- The conductivity ratio and density function also have a negative effect on the system stability i.e., both factors oppose the system stability and conductivity ratio is to advance the onset of convection.
- The effect of rotation of porous layer modified conductivity ratio is to enhance the heat transport.
- The overall conclusion is that the rotation parameter Ta stabilizes the system whereas the internal heat generation, conductivity ratio, and density function are having a destabilizing effect on the onset of convection.

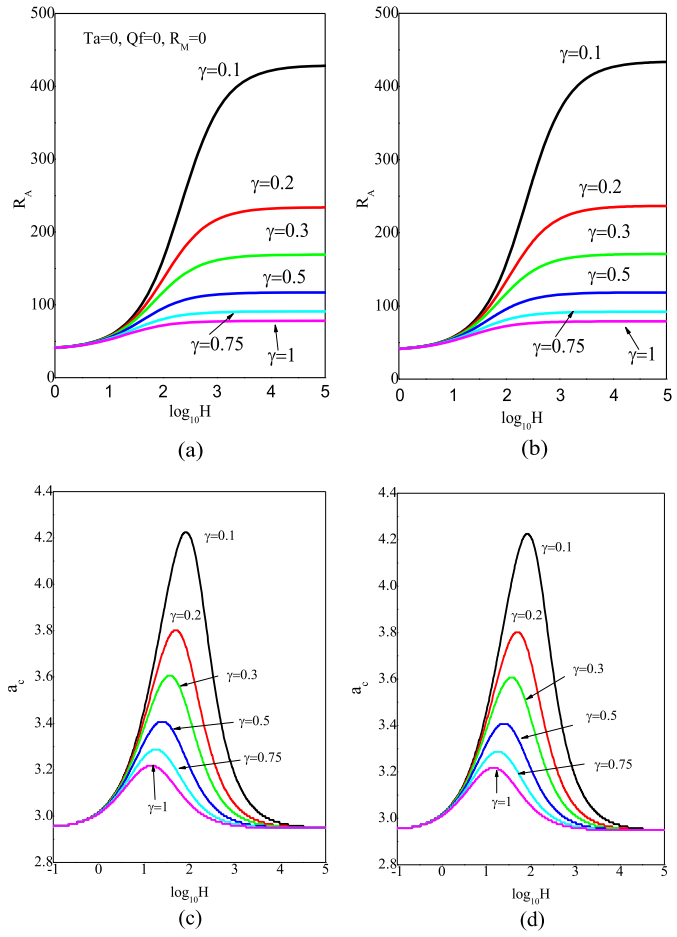

Fig. 6. (a): Variation of R_A v/s H for specific values of γ in present study. (b): Variation of R_A v/s H for different values of γ in DAS Rees et al. result. (c): Variation of ac v/s H for different value of γ in present study. (d): Variation of ac v/s H for different value of γ in Rees et al. result.

Table 2. Comparison of the critical wavenumber of present study with Darcy–Benard convection done by Banu and Rees [5] in the absence of rotation, internal heat generation and maximum density function.

Variation of critical wavenumber versus logH for specific values of g								
H	Present study				Banu and Rees [5]			
	$\gamma = 0.1$	$\gamma = 0.3$	$\gamma = 0.5$	$\gamma = 1$	$\gamma = 0.1$	$\gamma = 0.3$	$\gamma = 0.5$	$\gamma = 1$
-2	3.13958	3.13958	3.13958	3.13958	3.14643	3.14643	3.14643	3.14643
-1	3.14804	3.14804	3.14804	3.14804	3.14643	3.14643	3.14643	3.14643
0	3.14804	3.20662	3.20662	3.19832	3.21714	3.21714	3.21714	3.20936
1	3.14804	3.57378	3.50662	3.39936	3.69459	3.61939	3.55668	3.43511
2	3.14804	3.61783	3.40714	3.24778	4.61519	3.72156	3.46410	3.27109
3	3.14804	3.19832	3.17329	3.14804	3.42783	3.21714	3.18591	3.15436
4	3.14804	3.13958	3.13958	3.13958	3.17017	3.14643	3.14643	3.14643
5	3.14804	3.13958	3.13958	3.13958	3.14643	3.14643	3.13847	3.13847
6	3.14804	3.13958	3.13958	3.13958	3.13847	3.13847	3.13847	3.13847
7	3.14804	3.13958	3.13958	3.13958	3.13847	3.13847	3.13847	3.13847
8	3.14804	3.13958	3.13958	3.13958	3.13847	3.13847	3.13847	3.13847
9	3.14804	3.13958	3.13958	3.13958	3.13847	3.13847	3.13847	3.13847
10	3.14804	3.13958	3.13958	3.13958	3.13847	3.13847	3.13847	3.13847

Declarations

Author contribution statement

N.K. Enagi and Sridhar Kulkarni: Conceived and designed the experiments; Wrote the paper.

Krishna B. Chavaraddi and G.K. Ramesh: Analyzed and interpreted the data; Contributed reagents, materials, analysis tools or data; Wrote the paper.

Funding statement

This research did not receive any specific grant from funding agencies in the public, commercial, or not-for-profit sectors.

Data availability statement

Data included in article/supp. material/referenced in article.

Declaration of interests statement

The authors declare no conflict of interest.

Additional information

No additional information is available for this paper.

Acknowledgements

The Authors are very much thankful to the editor and reviewers for their thoughtful comments and constructive suggestions towards improving the presentation of this manuscript. The author (KBC) wishes to thank UGC and DCE, Government of Karnataka for encouragement and support. Also, the authors (NKE, SK and GKR) wish to thank respectively the management/Principal of their institutions for their encouragement and support in doing research.

References

[1] D.A. Nield, A. Bejan, Convection in Porous Media, 3rd ed., Springer, Berlin, 2006.
[2] D.A.S. Rees, I. Pop, Free convection in stagnation point flow in a porous medium using thermal non equilibrium model, Int. Commun. Heat Mass Transf. 26 (1999) 945–954.
[3] D.A.S. Rees, L. Storesletten, A. Postelnicu, The onset of convection in an inclined anisotropic porous layer with oblique principal axes, Transp. Porous Media 62 (2) (2006) 139–156.
[4] S. Govender, P. Vadasz, The effect of mechanical and thermal anisotropy on the stability of gravity driven convection in rotating porous media in the presence of thermal non-equilibrium, Transp. Porous Media 69 (1) (2007) 55–66.
[5] N. Banu, D.A.S. Rees, Onset of Darcy-Benard convection using a thermal non-equilibrium model, Int. J. Heat Mass Transf. 45 (2002) 2221–2228.
[6] M.S. Malashetty, I.S. Shivakumara, S. Kulkarni, The onset of convection in an anisotropic porous layer using a thermal non-equilibrium model, Transp. Porous Media 51 (2005) 1–17.
[7] M.S. Malashetty, I.S. Shivakumara, Sridhar Kulkarni, Convective instability of Oldroyd-B fluid saturated porous layer heated from below using a thermal non-equilibrium model, Transp. Porous Media 64 (2006) 123–139.
[8] M.S. Malashetty, I.S. Shivakumara, S. Kulkarni, The onset of convection in a couple stress fluid saturated porous layer using a thermal non equilibrium model, Phys. Lett. A 373 (7) (2009) 781–790.
[9] M.S. Malashetty, I.S. Shivakumara, S. Kulkarni, The onset of Lapwood-Brinkman convection using a thermal non-equilibrium model, Int. J. Heat Mass Transf. 48 (6) (2005) 1155–1163.
[10] M.S. Malashetty, M. Swamy, S. Kulkarni, Thermal convection in a rotating porous layer using a thermal non-equilibrium model, Phys. Fluids 19 (5) (2007) 054102.
[11] A. Postelnicu, Effect of inertia on the onset of mixed convection in a porous layer using thermal non equilibrium model, J. Porous Media 10 (50) (2007) 515–524.
[12] A.V. Kuznetsov, D.A. Nield, Effect of local thermal non-equilibrium on the onset of convection in a porous medium layer saturated by a nanofluid, Transp. Porous Media 2 (83) (2010) 425–436.
[13] V. Yekasi, S. Pranesh, Effect of suction-injection combination and internal heat source in a fluid with internal angular momentum under 1g and μg, J. Comput. Math. Sci. 9 (6) (2018) 526–537.
[14] B.S. Bhadauria, I. Hashim, P.G. Siddeshwar, Effect of internal heating on weakly nonlinear stability analysis of Rayleigh-Benard convection under g-jitter, Int. J. Non-Linear Mech. 54 (2013) 35–42.
[15] I.S. Shivakumara, M.S. Malashetty, K.B. Chavaraddi, Onset of convection in a visco-elastic-fluid-saturated sparsely packed porous layer using a thermal non equilibrium model, Can. J. Phys. 84 (11) (2006) 973–990.
[16] I.S. Shivakumara, A.L. Mamatha, M. Ravisha, Boundary and thermal non-equilibrium effects on the onset of Darcy-Brinkman convection in a porous layer, J. Eng. Math. 67 (2010) 317–328.
[17] I.S. Shivakumara, A.L. Mamatha, M. Ravisha, Effects of variable viscosity and density maximum on the onset of Darcy-Benard convection using a thermal non equilibrium model, J. Porous Media 13 (7) (2010) 613–622.
[18] Jinho Lee, I.S. Shivakumara, M. Ravisha, Effect of thermal non-equilibrium on convective instability in a ferromagnetic fluid saturated porous medium, Transp. Porous Media 86 (2011) 103–124.
[19] I.S. Shivakumara, Jinho Lee, M. Ravisha, R. Gangadhara Reddy, The onset of Brinkman ferro convection using a thermal non-equilibrium model, Int. J. Heat Mass Transf. 54 (2011) 2116–2125.
[20] I.S. Shivakumara, Jinho Lee, A.L. Mamatha, M. Ravisha, Boundary and thermal non-equilibrium effects on convective instability in an anisotropic porous layer, J. Mech. Sci. Technol. 25 (2011) 911–921.
[21] I.S. Shivakumara, R. Gangadhara Reddy, M. Ravisha, Jinho Lee, Effect of rotation on ferromagnetic porous convection with a thermal non-equilibrium model, Meccanica 49 (2014) 1139–1157.
[22] I.S. Shivakumara, M. Ravisha, C.O. Ng, V.L. Varun, A thermal non-equilibrium model with Cattaneo effect for convection in a Brinkman porous layer, Int. J. Non-Linear Mech. 71 (2015) 39–47.
[23] D. Yadav, J. Wang, Jinho Lee, Onset of Darcy–Brinkman convection in a rotating porous layer induced by purely internal heating, J. Porous Media 20 (8) (2017) 691–706.
[24] S. Sarvanan, Thermal non-equilibrium porous medium with heat generation and density maximum, Transp. Porous Media 76 (2009) 35–43.
[25] R.D. Gaseer, M.S. Kazimi, Onset of convection in a porous media with internal heat generation, J. Heat Transf. 98 (10) (1976) 49–54.
[26] K.B. Chavaraddi, N.K. Enagi, S. Kulkarni, Onset of convection in a couple stress fluid saturated rotating anisotropic porous layers using thermal non-equilibrium model, J. P. J. Heat Mass Transf. 16 (1) (2019) 125–142.
[27] L.S. Lotten, D.A.S. Rees, Onset of convection in an inclined anisotropic porous layer with internal heat generation, Fluids 4 (2019) 75.
[28] C. Israel-Cookey, V.B. Omubo-Peppl, Onset of thermal instability in a low Prandtl number fluid with internal heat source in a porous medium, Am. J. Sci. Ind. Res. 1 (1) (2010) 18–24.
[29] A.K. Srivastava, B.S. Bhadauria, J. Kumar, Magneto convection in an anisotropic porous layer using thermal non-equilibrium model, Special topics & reviews in Porous Media 1 (2) (2011) 1–10.
[30] A. Postelnicu, Effect of inertia on the onset of mixed convection in a porous layer using thermal non-equilibrium model, J. Porous Media 10 (5) (2007) 515–524.

[31] X.J. Xu, Z.B. Xing, F.Q. Wang, Z.M. Cheng, Review on heat conduction, heat convection, thermal radiation and phase change heat transfer of nanofluids in porous media: fundamentals and applications, Chem. Eng. Sci. 195 (2019) 462–483.
[32] M.E.H. Oumar, S.N. Arshika, S. Pranesh, The effect of internal heat generation on the onset of Rayleigh-Benard electro-convection in a micropolar fluid, Int. J. Appl. Eng. Res. 14 (2019) 2327–2335.
[33] C.Q. Wu, H.J. Xu, C.Y. Zhao, A new fractal model on fluid flow/heat/mass transport in complex porous structures, Int. J. Heat Mass Transf. 162 (2020) 120292.
[34] H.J. Xu, Thermal transport in microchannels partially filled with micro-porous media involving flow inertia, flow/thermal slips, thermal non-equilibrium and thermal asymmetry, Int. Commun. Heat Mass Transf. 110 (2020) 104404.
[35] A.A. Yousif, Omar Rafae Alomar, A.T. Hussein, Impact of using triple adiabatic obstacles on natural convection inside porous cavity under non-Darcy flow and local thermal non-equilibrium model, Int. Commun. Heat Mass Transf. 130 (2022) 105760.
[36] Omar Rafae Alomar, Miguel Mendes, D. Trimis, Subhashis Ray, Simulation of complete liquid–vapour phase change process inside porous evaporator using local thermal non-equilibrium model 94 (2015) 228–241.
[37] Omar Rafae Alomar, Analysis of variable porosity, thermal dispersion, and local thermal non-equilibrium on two-phase flow inside porous media 154 (2019) 263–283.
[38] Omar Rafae Alomar, Miguel Mendes, D. Trimis, S. Ray, Numerical simulation of complete liquid–vapour phase change process inside porous media: a comparison between local thermal equilibrium and non-equilibrium models 112 (2017) 222–241.